AD-A035 817 AEROSPACE CORP EL SEGUNDO CALIF IVAN A GETTING LABS F/G 20/6
SHORT-TERM AVERAGE IRRADIANCE PROFILE OF AN OPTICAL BEAM IN A T--ETC(U)
JAN 77 M T TAVIS, H T YURA F04701-76-C-0077
UNCLASSIFIED TR-0077(2608)-1 SAMSO-TR-77-27 NL

1 OF 1
ADA035817

END

DATE
FILMED
3 - 77

REPORT SAMSO-TR-77-27

Short-Term Average Irradiance Profile of an Optical Beam in a Turbulent Medium

Electronics Research Laboratory
The Ivan A. Getting Laboratories
The Aerospace Corporation
El Segundo, Calif. 90245

28 January 1977

Interim Report

Prepared for
SPACE AND MISSILE SYSTEMS ORGANIZATION
AIR FORCE SYSTEMS COMMAND
Los Angeles Air Force Station
P.O. Box 92960, Worldway Postal Center
Los Angeles, Calif. 90009

This report was submitted by The Aerospace Corporation, El Segundo, CA 90245, under Contract F04701-76-C-0077 with the Space and Missile Systems Organization, Deputy for Advanced Space Programs, P.O. Box 92960, Worldway Postal Center, Los Angeles, CA 90009. It was reviewed and approved for The Aerospace Corporation by A. H. Silver, Director, Electronics Research Laboratory. Lieutenant Ronald C. Lawson, SAMSO/YAPT, was the project engineer.

This report has been reviewed by the Information Office (OI) and is releasable to the National Technical Information Service (NTIS). At NTIS, it will be available to the general public, including foreign nations.

This technical report has been reviewed and is approved for publication. Publication of this report does not constitute Air Force approval of the report's findings or conclusions. It is published only for the exchange and stimulation of ideas.

FOR THE COMMANDER

Ronald C Lawson

Ronald C. Lawson, 1st Lt. USAF
Technology Plan Division
Deputy for Advance Space Program

UNCLASSIFIED

SECURITY CLASSIFICATION OF THIS PAGE (When Data Entered)

(19) REPORT DOCUMENTATION PAGE		READ INSTRUCTIONS BEFORE COMPLETING FORM
1. REPORT NUMBER (18) SAMSO TR-77-27	2. GOVT ACCESSION NO.	3. RECIPIENT'S CATALOG NUMBER
4. TITLE (and Subtitle) (6) SHORT-TERM AVERAGE IRRADIANCE PROFILE OF AN OPTICAL BEAM IN A TURBULENT MEDIUM.		5. TYPE OF REPORT & PERIOD COVERED (9) Technical Rept.
		6. PERFORMING ORG. REPORT NUMBER (14) TR-0077(2608)-1
7. AUTHOR(s) (10) M. T. Tavis and H. T. Yura		8. CONTRACT OR GRANT NUMBER(s) (15) F04701-76-C-0077
9. PERFORMING ORGANIZATION NAME AND ADDRESS (1) The Aerospace Corporation (2) El Segundo, Calif. 90245 (3) Edwin A. Stuhring Labs		10. PROGRAM ELEMENT, PROJECT, TASK AREA & WORK UNIT NUMBERS (12) 48p.
11. CONTROLLING OFFICE NAME AND ADDRESS (11) Space and Missile Systems Organization, Air Force Systems Command, Los Angeles, Calif. 90009		12. REPORT DATE 28 Jan 77
		13. NUMBER OF PAGES 45
14. MONITORING AGENCY NAME & ADDRESS (If different from Controlling Office)		15. SECURITY CLASS. (of this report) Unclassified
		15a. DECLASSIFICATION/DOWNGRADING SCHEDULE

16. DISTRIBUTION STATEMENT (of this Report)

Approved for public release; distribution unlimited

17. DISTRIBUTION STATEMENT (of the abstract entered in Block 20, if different from Report)

18. SUPPLEMENTARY NOTES

19. KEY WORDS (Continue on reverse side if necessary and identify by block number)

Irradiance
Mutual coherence function
Optical propagation
Short term beam
Turbulence theory

20. ABSTRACT (Continue on reverse side if necessary and identify by block number)

The short-term average irradiance profile of a focused laser beam transmitted through a homogeneous-isotropic medium has been determined by using the extended Huygens-Fresnel principle and by modifying the phase structure function to remove tilt. In contrast to previous analysis, no assumption is made regarding the independence of the distribution of phase with tilt removed and the random vector $\vec{\beta}$ defining tilt. This analysis applies to the near field of the effective coherent transmitting aperture,

→ Next page

DD FORM (FACSIMILE) 1473

409 944 ✓

UNCLASSIFIED

SECURITY CLASSIFICATION OF THIS PAGE (When Data Entered)

19. KEY WORDS (Continued)

20. ABSTRACT (Continued)

where the beam wanders as a whole and does not break up into multiple patches or blobs. Central to the analysis is the short-term average mutual coherence function (MCF) of a spherical wave which has been determined from the modified phase structure function. Assuming a Kolmogorov spectrum, the modified phase structure function has been determined for three specific aperture functions. These same aperture functions are then used to determine the short-term irradiance profiles. Numerical calculations have been performed and the results are presented for uniform and gaussian aperture functions for various values of aperture obscuration and for various strengths of turbulence values. Comparisons are made between the long-term average, short-term average, and Fried's short-term average irradiance profiles. In particular, on axis irradiance values and beam spread, as determined by the 1/e points in irradiance, are compared. It is found, in contrast to previous analysis, that the short-term beam spread remains relatively constant as the strength of turbulence becomes large and then increases slowly.

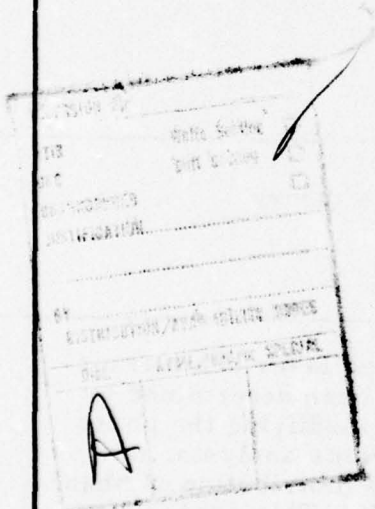

CONTENTS

FIGURES

FIGURES (Continued)

Introduction

Many laser systems operating in the atmosphere can be degraded by atmospheric turbulence. For example, target-illumination systems, communication systems, radar systems, and others may be severely affected by turbulence effects which include beam spreading and scintillation. Since beam spreading and its associated on-axis irradiance degradations are of practical interest, a detailed theoretical description of the improved on-target irradiance characteristics resulting from cancellation of turbulence-induced beam wander effects is desired. Previous treatments[1-4] of the atmospheric induced laser beam spreading have been concerned mainly with the determination of the long-term average beam spread, i.e., the effects of both beam breathing and wander are included.

A previous semi-quantitative analysis[5] indicates that the short-term average beam spread (beam spread with a wander correction) rapidly approaches the long-term average beam spread as the strength of turbulence increases. This is contrary to the result of recent unpublished experiments[6] and the theoretical analysis presented below. Rather than treating the short-term average beam spread alone, the complete analytic expressions for the short-term average (i.e., beam wander cancelled) irradiance profile of a focused laser beam transmitted through isotropic homogeneous turbulence for a general aperture distribution (and in particular for three specified aperture functions) will be derived. Then, short-term laser beam spread may easily be determined from the 1/e value in irradiance.

Following previous discussions,[5, 7] an optical beam interacts with atmospheric refractive inhomogeneities of all scales. Turbulent eddies having characteristic dimensions greater than the beam diameter

lead to refractive effects (beam wander); these large-scale inhomogeneities lead to net wavefront tilt. In this case, there is no beam breathing and the only effect is that the entire beam dances around its unperturbed position. Conversely, eddies having characteristic dimensions less than the beam diameter lead to diffractive effects (breathing) about the instantaneous center of energy. The term long-term-average is used to imply averages over a time long compared with all fluctuations of interest (i.e., over all possible ensembles that the index-of-refraction fluctuations can possibly assume). This means that the effects of beam tilt (wander) and beam breathing are included in the analysis of the propagation problem when the long-term average is taken. Here, however, we are concerned with the short-term average irradiance profile about the instantaneous center of energy of the focused beam. This case is of physical interest when the beam dances as a whole and does not break up into multiple blobs, i.e., when amplitude fluctuations are small as in the near field of the effective coherent transmitting aperture. This is equivalent to the requirement that the propagation distance $z << k\ell^2$ where k is the optical wave number and ℓ the smaller of the initial transmitted beam diameter (D) or the long-term spherical wave lateral coherence length[5] (ρ_o). This is equivalent to the statement that the variance in the log-amplitude of a spherical wave is much less than unity $\langle \chi_s^2 \rangle << 1$. (Sharp angular brackets denote the ensemble average and we will drop the subscript s, indicating spherical wave, in the remainder of this paper.) Finally, since turbulent eddies of characteristic dimensions greater than the beam diameter D are responsible for producing tilt, the short-term average will imply averages performed over a time

shorter than D/V_n, where V_n is the normal wind velocity (i.e., assuming a frozen turbulence model). This indicates that the short-term average excludes the effect of beam wander.

General considerations regarding the irradiance profile are discussed in Section I, where it is shown how the short-term average irradiance profile depends on the modified phase structure function. In Section II, this modified, or short-term average, structure function and therefore the mutual coherence function (MCF) of a spherical wave is shown to be a function of not only the difference coordinate ($\vec{\rho}$), of two arbitrary points in the aperture, but is also a function of the corresponding sum coordinate ($\vec{R}$). This is contrary to the results employed by Fried[7] where statistical independence of phase with tilt removed and the random vector $\vec{\beta}$ defining tilt was assumed. To proceed further, a Kolmogorov spectrum of turbulence is assumed and three specific forms for an aperture function are employed to determine the modified MCF. Using the modified MCF, expressions for the short-term average irradiance profiles are presented in Section III. The aperture functions U_A considered are uniform with finite cutoff and obscuration, gaussian with finite cutoff and obscuration, and infinite gaussian with semi-gaussian obscuration. A numerical example is provided for the case of the truncated gaussian with obscuration for various values of normalized strength of turbulence (ε) varying between 0.1 and 10.0 where $\varepsilon = D/\rho_o$. For comparison the long-term irradiance profiles will be exhibited for the same cases. Plots comparing the center of energy irradiance values and beam half width for various cases are also presented.

The present analysis is restricted to a weakly inhomogeneous medium with characteristic scale lengths much greater than the optical wavelength. In addition, it is assumed that the characteristics of the medium do not change appreciably during an oscillation period of the optical field at infrared and visible wavelengths. This condition is well satisfied in the atmosphere. The electromagnetic field considered has a time dependence given by the multiplicative factor $\exp(-i\omega t)$. The time-dependent wave equation is replaced by the Helmholtz equation for an inhomogeneous medium having an electrical conductivity and magnetic permeability equal to zero and one, respectively. Only the case of the propagation of a scalar field in a fluctuating medium is discussed. Profiles are calculated at the focal point with extension to non-focal points being straightforward though nontrivial. For simplicity a spatially homogeneous turbulent medium is assumed.

I. General Considerations

The short-term, long-term, and Fried's approximation* to be short-term irradiance profile are obtained from the extended Huygens-Fresnel principle of Lutomirski and Yura[2]. From this principle, the instantaneous field due to an arbitrary complex aperture distribution can be computed by superimposing wavelets that radiate from all elements of the aperture. The properties of the medium appear only in the propagation properties of the spherical wavelets thus separating the geometry of the problem (aperture distribution) from the propagation problem. The instantaneous irradiance at a point $\vec{p}$ located in the plane perpendicular to the z-axis at a propagation distance z from a transmitting aperture is,

*The use of the words "Fried's approximation" is used in the context that one employs the approximations made in Ref. (7) for the modulation transfer function (MTF) to the MCF used here to find the irradiance profile. Fried never made beam calculations, he calculated the MTF in short exposure imagery.

in the paraxial approximation[2],

$$I(\vec{p}) = E\left(\frac{k}{2\pi z}\right)^2 \iint \exp\left[-\frac{ik\vec{p}\cdot(\vec{r}_1 - \vec{r}_2)}{z}\right] \exp\left[-\frac{ik}{2}\left(\frac{1}{f} - \frac{1}{z}\right)\left(r_1^2 - r_2^2\right)\right]$$
$$\times \exp\left[\psi(\vec{r}_1) + \psi^*(\vec{r}_2)\right] U_A(\vec{r}_1)\, U_A^*(\vec{r}_2)\, d^2\vec{r}_1\, d^2\vec{r}_2 \qquad (1)$$

where $U_A(\vec{r}_1)$ is the specified initial complex aperture amplitude distribution, $\psi(\vec{r}_1)$ and $\psi(\vec{r}_2)$ are the perturbations in the field at $\vec{p}$ due to the atmosphere for unit spherical waves propagated from $\vec{r}_1$ and $\vec{r}_2$, f is the focal range, k is the propagation constant $2\pi/\lambda$ with λ the wavelength, and for convenience the constant E is chosen such that the total power transmitted through the aperture is a constant irrespective of obscuration or type of aperture function.

In Eq. (1) we have neglected derivatives of the perturbations ψ with respect to the propagation distance as they are small quantities compared to k.[2] After an average is performed over a time that is long compared with all fluctuation periods of interest (over all possible ensembles that the index-of-refraction fluctuations can possible assume), the long-term (LT) mean irradiance profile [for the focused case (f = z)] is obtained from Eq. (1) as

$$\langle I(\vec{p})\rangle_{LT} = E\left(\frac{k}{2\pi z}\right)^2 \iint \exp\left[-\frac{ik\vec{p}\cdot(\vec{r}_1 - \vec{r}_2)}{z}\right] M_{LT}(\vec{r}_1, \vec{r}_2, z)$$
$$\times U_A(\vec{r}_1)\, U_A^*(\vec{r}_2)\, d^2\vec{r}_1\, d^2\vec{r}_2 \qquad (2)$$

where M_{LT} is the long-term MCF of a spherical wave located at the point $\vec{p}$ and observed in the aperture plane at $\vec{r}_1$ and $\vec{r}_2$.[2] For the case of homogeneous isotropic turbulence

$$M_{LT}(\vec{r}_1, \vec{r}_2, z) = M_{LT}(\rho, z) = \exp\left[-\frac{1}{2} D_\psi(\rho, z)\right] \quad (3)$$

where ρ is the magnitude of $\vec{\rho} = \vec{r}_1 - \vec{r}_2$ and $D_\psi(\rho, z)$ is the wave structure function defined as the sum of log-amplitude and phase structure functions:[8]

$$D_\psi = D_\chi(\rho, z) + D_\phi(\rho, z) \quad (4)$$

For the Kolmogorov spectrum in the inertial subrange, it has been shown[5] that

$$D_\psi = 2(\rho/\rho_o)^{5/3} \quad (5)$$

where ρ_o is the LT lateral coherence length defined in Eq. (14) of Ref. 1. It can be shown[9] that the phase-structure function $D_\phi(\rho)$ (we drop the explicit z dependence) can be written as

$$D_\phi = \alpha(\rho) D_\psi(\rho)$$

where $\alpha(\rho)$ varies smoothly between 1 for $z \ll k\rho^2$ to 1/2 for $z \gg k\rho^2$. In this paper we have already assumed that $z \ll k\ell^2$ which implies that for all significant values of ρ, $\alpha(\rho) = 1$ and that the log-amplitude variance $\langle\chi^2\rangle \ll 1$.

What is of more interest here, however, is the irradiance distribution obtained on a short-term basis for which the tilt of the wavefront has been removed, for example by reciprocity tracking. This is accomplished by formulation of a precise statistical definition of the deformed wavefront "shape" in terms of a series of polynomials, as defined by Fried.[10] The instantaneous wavefront tilt can be represented in terms of linear polynomials and this tilt is removed from the

wavefront phase by defining

$$\gamma(\vec{r}) = \phi(\vec{r}) - \vec{\beta} \cdot \vec{r} \tag{6}$$

where $\vec{\beta}$ is a random vector related to $\phi(\vec{r})$ in such a manner that $\vec{\beta} \cdot \vec{r}$ gives the best fit to $\phi(\vec{r})$ in terms of a least-squares difference over the aperture,[10] i.e.

$$\frac{\partial}{\partial \beta_i} \int d^2\vec{r}\, W(\vec{r}) [\phi(\vec{r}) - \vec{\beta} \cdot \vec{r}]^2 = 0 \tag{7}$$

This implies that the i-th component of the vector defining tilt (i = x, y) is

$$\beta_i = \frac{\int r_i \phi(\vec{r})\, W(\vec{r})\, d^2\vec{r}}{\int r_i^2\, W(\vec{r})\, d^2\vec{r}} \tag{8}$$

where $W(\vec{r})$ is a real aperture function defined such that W is porportional to $|U_A(\vec{r})|^2$. It is not necessary to normalize W as the normalization factor cancels in the definition of β_i (Eq. 8). The above choice for W was made to maximize tilt removal. Other choices were considered during this study but were found to give non-optimum results. With tilt removed the resulting beam profile is determined by the geometry of the problem (the arbitrary complex aperture distribution) and the propagation problem (diffractive scattering by eddies having characteristic dimensions less than the order of the beam diameter). The use of the extended Huygens-Fresnel principle separates these two problems.

Averaging Eq. (1) for times short compared to D/v_n, the short-term (ST) irradiance profile is obtained for f = z as

$$\langle I(\vec{p})\rangle_{ST} = E\left(\frac{k}{2\pi z}\right)^2 \iint \exp\left[-\frac{ik\vec{p}\cdot(\vec{r}_1 - \vec{r}_2)}{z}\right] M_{ST}(\vec{r}_1, \vec{r}_2)$$

$$\times U_A(\vec{r}_1)\, U_A^*(\vec{r}_2)\, d^2\vec{r}_1\, d^2\vec{r}_2 \tag{9}$$

where

$$M_{ST}(\vec{r}_1, \vec{r}_2) = \langle \exp[\psi(\vec{r}_1) + \psi^*(\vec{r}_2) - i\vec{\beta}\cdot(\vec{r}_1 - \vec{r}_2)]\rangle \tag{10}$$

is the "*effective short-term*" average MCF of a spherical wave located at point $\vec{p}$ observed in the plane of the transmitting aperture.

II. Short Term Average MCF

To be general, Eq. (10) is rewritten to exhibit the dependence on phase and log-amplitude:

$$M_{ST}(\vec{r}_1, \vec{r}_2) = \langle \exp\left|\chi(\vec{r}_1) + \chi(\vec{r}_2) + i[\phi(\vec{r}_1) - \phi(\vec{r}_2) - \vec{\beta}\cdot(\vec{r}_1 - \vec{r}_2)]\right| \rangle \tag{11}$$

As in Ref. 7 it is assumed that $\vec{\beta}$, like χ and ϕ, is normally distributed. Furthermore, the distribution of $[\phi(\vec{r}_1) - \phi(\vec{r}_2) - \vec{\beta}\cdot(\vec{r}_1 - \vec{r}_2)$ is independent of the distribution of $[\chi(\vec{r}_1) + \chi(\vec{r}_2)]$, since we have assumed that the turbulence is locally isotropic and homogeneous. In contrast to Ref. 7, it is not assumed here that the distribution of $\vec{\beta}$ is independent of the distribution of $[\phi(\vec{r}) - \vec{\beta}\cdot\vec{r}]$. Using conservation of energy, it is then easy to show that

$$M_{ST}(\vec{r}, \vec{r}_2) = \exp\left|-\frac{1}{2}[D_\chi(\rho) + D_\gamma(\vec{r}_1, \vec{r}_2)]\right| \tag{12}$$

where $D_\gamma(\vec{r}_1, \vec{r}_2)$ the modified phase structure, given by

$$D_\gamma(\vec{r}_1, \vec{r}_2) = \langle[\gamma(\vec{r}_1) - \gamma(\vec{r}_2)]^2\rangle \tag{13}$$

$$= \langle[\phi(\vec{r}_1) - \phi(\vec{r}_2)]^2\rangle + \langle(\vec{\beta}\cdot\vec{\rho})^2\rangle - 2\vec{\rho}\cdot\langle\vec{\beta}[\phi(\vec{r}_1) - \phi(\vec{r}_2)]\rangle$$

Substituting Eq. (8) into Eq. (13) and assuming that the aperture function W is circularly symmetric, the modified phase structure function is given by

$$D_\nu(\vec{r}_1, \vec{r}_2) = D_\phi(\rho) - \frac{A^2}{2} \iint (\vec{\rho}\cdot\vec{r})(\vec{\rho}\cdot\vec{r}')\, W(r)\, W(r')\, D_\phi(|\vec{r} - \vec{r}'|)\, d^2r\, d^2r' + A\vec{\rho}\cdot\left[\int \vec{r}\, W(r)\, D_\phi(|\vec{r} - \vec{r}_1|)\, d^2r - \int \vec{r}\, W(r)\, D_\phi(|\vec{r} - \vec{r}_2|)\, d^2r\right], \tag{14}$$

where

$$A = \left(\pi \int r^3\, W(r)\, dr\right)^{-1} . \tag{15}$$

Equation 14 may be rewritten through the use of symmetry in the angular variable as

$$D_\nu(\vec{\rho}, \vec{R}) = D_\phi(\rho) - \frac{A^2}{4}\rho^2 \iint (\vec{r}\cdot\vec{r}')\, W(r)\, W(r')\, D_\phi(|\vec{r} - \vec{r}'|)\, d^2\vec{r}\, d^2\vec{r}' + A\left[\frac{(\vec{r}_1\cdot\vec{\rho})}{r_1^2}\int \vec{r}_1\cdot\vec{r}\, W(r)\, D_\phi(|\vec{r} - \vec{r}_1|)\, d^2r - \frac{(\vec{r}_2\cdot\vec{\rho})}{r_2^2}\int \vec{r}_2\cdot\vec{r}\, W(r)\, D_\phi(|\vec{r} - \vec{r}_2|)\, d^2r\right] \tag{16}$$

where $\vec{R} = \frac{\vec{r}_1 + \vec{r}_2}{2}$ and as above $\vec{\rho} = \vec{r}_1 - \vec{r}_2$. Note that the factor multiplying ρ^2 in Eq. (16) is a constant while the factors multiplying $\vec{\rho}\cdot\vec{r}_1$ and $\vec{\rho}\cdot\vec{r}_2$ are functions of only $\vec{r}_1$ and $\vec{r}_2$, respectively. The "effective" short-term structure function is given by $D_\chi + D_\nu = D_\psi + \Delta$, where D_ψ is the long-term wave structure function and Δ represents the effects of tilt removal and is given explicitly by the integral terms in Eq. (16). The details of obtaining the short-term spherical wave MCF for specific choices of W is left to the Appendix.

III. Irradiance Profiles for Specified Aperture Distributions

In this section the expressions for the short-term irradiance profiles for a focused beam transmitted through isotropic homogeneous turbulence is presented for the case of a truncated-obscured uniform amplitude aperture distribution, the case of a truncated-obscured gaussian amplitude aperture distribution with a gaussian intensity halfwidth of α_o, and the case of an infinite gaussian with a gaussian halfwidth given by b and with semi-gaussian obscuration. (The expression for the amplitude aperture distribution for this case is given by

$$U_A = Q_1 \; e^{-r^2/2b^2} \left(1 - e^{-r^2/a^2}\right)$$

where Q_1 is a constant determined by the normalization of the irradiance profile). The three cases above are designated by the symbol ν (= 1, 2, 3). For cases ν = 1, 2 the truncation and obscuration radii are given by b and a, respectively. These amplitude aperture functions and the corresponding effective short-term MCF are substituted into Eq. (9) to obtain the irradiance profiles. To simplify the expression, a change of integration variables in Eq. (9) is made from $\vec{r}_1$ and $\vec{r}_2$ to the sum and difference coordinates $\vec{R}$ and $\vec{\rho}$. Further, the integrals are made dimensionless and dimensional factors are included into the constant E. To accomplish this, $\vec{R}$ is divided by b and $\vec{\rho}$ by 2b. Although the same symbols will be used in the integration to determine irradiance, they are now dimensionless. The short-term MCF corresponding to the three aperture distributions is given in terms of the dimensionless $\vec{\rho}$, $\vec{R}$ from Eqs. (12) and (16) by

$$M_{ST\,\nu}(\vec{\rho}, \vec{R}) = \exp\Big\{ - \varepsilon^{5/3} (\rho^{5/3} + C_\nu \rho^2) + \left(\frac{\varepsilon}{2}\right)^{5/3} [\vec{\rho} \cdot \vec{r}_1 \, G_\nu(r_1) - \vec{\rho} \cdot \vec{r}_2 \, G_\nu(r_2)] \Big\} \tag{17}$$

where $\varepsilon = 2b/\rho_o$, $\vec{r}_1 = \vec{R} + \vec{\rho}$ and $\vec{r}_2 = \vec{R} - \vec{\rho}$, C_ν and $G_\nu(x)$ are given in the Appendix, and the Kolmogorov spectrum of turbulence is assumed. Note that for the Kolmogorov spectrum, the long-term average MCF is obtained from Eq. (17) by setting both C_ν and $G_\nu = 0$ while Fried's approximation[7] to the short-term average MCF may be obtained from Eq. (17) by changing the sign of C_ν and setting $G_\nu = 0$.

The expressions for the short-term average focused irradiance profiles for cases $\nu = 1, 2$ are obtained from Eqs. (9) and (17) in a manner similar to that used in the Appendix for obtaining the quantity C_ν and are presented without further comment

$$\langle I_\nu(\vec{\rho}) \rangle_{ST} = \frac{P}{\pi b^2} \left(\frac{\pi b^2}{\lambda z}\right)^2 \left\{ \frac{32}{\pi} \, S_\nu \right.$$

$$\times \left[\int_0^1 B_\nu(\rho) \, \rho d\rho \int_0^{\cos^{-1}\rho} d\theta \int_{\rho \sec\theta}^1 H_\nu(\vec{\rho}, \vec{R} - \vec{\rho}) \, R dR \right.$$

$$\left. + \int_0^\delta B_\nu(\rho) \, \rho d\rho \int_0^{\cos^{-1}\frac{\rho}{\delta}} d\theta \int_{\rho \sec\theta}^\delta H_\nu(\vec{\rho}, \vec{R} - \vec{\rho}) \, R dR \right]$$

$$- \int_0^{\frac{1+\delta}{2}} B_\nu(\rho)\, \rho d\rho \int_0^{\pi} d\theta \int_0^{\delta} H_\nu(\vec{\rho},\, \vec{R} + \vec{\rho})\, R dR$$

$$+ \int_{\frac{1-\delta}{2}}^{\frac{1+\delta}{2}} B_\nu(\rho)\, \rho d\rho \left(\int_0^{\alpha} d\theta \int_0^{\delta} H_\nu(\vec{\rho},\, \vec{R} + \vec{\rho})\, R dR \right. \tag{18}$$

$$\left. \left. - \int_0^{\bar{\theta}} d\theta \int_{2\rho \sin\alpha \csc\varphi}^{1} H_\nu(\vec{\rho},\, \vec{R} - \vec{\rho})\, R dR \right) \right] \Bigg\} ,$$

where

$$B_1(\rho) = J_0\left(\frac{2kpb\rho}{z}\right) \exp\left[- \varepsilon^{5/3} \left(\rho^{5/3} + C_1 \rho^2 \right) \right] ,$$

$$B_2(\rho) = J_0\left(\frac{2kpb\rho}{z}\right) \exp\left[- \varepsilon^{5/3} \left(\rho^{5/3} + C_2 \rho^2 \right) \right] \quad e^{-\beta_o^2 \rho^2} ,$$

$$H_1(\vec{\rho}, \vec{R}) = \exp\left\{ \left(\frac{\varepsilon}{2}\right)^{5/3} \left[\vec{\rho} \cdot \vec{r}_1\, G_1(r_1) - \vec{\rho} \cdot \vec{r}_2\, G_1(r_2) \right] \right\} ,$$

$$H_2(\vec{\rho}, \vec{R}) = \exp\left\{ \left(\frac{\varepsilon}{2}\right)^{5/3} \left[\vec{\rho} \cdot \vec{r}_1\, G_2(r_1) - \vec{\rho} \cdot \vec{r}_2\, G_2(r_2) \right] \right\} e^{-\beta_o^2 R^2}$$

$$S_1 = (1 - \delta^2)^{-1} ,$$

$$S_2 = \beta_o^2 \left[e^{-(\delta\theta_o)^2} - e^{-\beta_o^2} \right]^{-1} ,$$

$$\alpha = \cos^{-1}\left(\frac{1 - 4\rho^2 - \delta^2}{4\delta\rho}\right) ,$$

$$\theta = \cos^{-1}\left(\frac{1 + 4\rho^2 - \delta^2}{4\rho}\right) ,$$

$$\varphi = \alpha - \theta, \quad \delta = a/b ,$$

$\beta_o = b/\alpha_o$ is the ratio of the aperture radius to the transmitted gaussian intensity halfwidth, P is the total power transmitted through the aperture, G_1, C_1, G_2, and C_2 are defined in Eqs. (A.8), (A.17), (A.20), (A.21), respectively and the angle between $\vec{\rho}$ and $\vec{R}$ is denoted by θ.

For the case of the infinite gaussian ($\nu = 3$), the short-term irradiance profile is given by

$$\langle I_3(p)\rangle_{ST} = \frac{P}{\pi b^2}\left(\frac{\pi b^2}{\lambda z}\right)^2 \left\{\frac{32}{\pi} S_3 \int_0^\infty J_0\left(\frac{2kbp\rho}{z}\right) \exp\left[-\epsilon^{5/3}\left(\rho^{5/3} + C_3\rho^2\right)\right]\right.$$

$$\times \left[e^{-\rho^2}\int_0^\infty e^{-R^2} RdR \int_0^{\pi/2} H_3(\vec{\rho}, \vec{R})\, d\theta\right.$$

$$- e^{-\rho^2}\int_0^\infty e^{-R^2} RdR \int_0^{\pi/2}\left(e^{-(R+\rho)^2\delta^2} + e^{-(R-\rho)^2\delta^2}\right) H_3(\vec{\rho}, \vec{R})\, d\theta \qquad (19)$$

$$\left.\left. + e^{-\left(\frac{\rho b}{e}\right)^2}\int_0^\infty e^{-\left(\frac{Rb}{e}\right)^2} RdR \int_0^{\pi/2} H_3(\vec{\rho}, \vec{R})\, d\theta\right] \rho\, d\rho\right\}$$

where

$$H_3 = \exp\left[\left(\frac{\epsilon}{2}\right)^{5/3}\left(G_3(r_1)\,\vec{\rho}\cdot\vec{r}_1 - G_3(r_2)\,\vec{\rho}\cdot\vec{r}_2\right)\right] ,$$

$$S_3 = \left[1 - 2\left(\frac{c}{b}\right)^2 + \left(\frac{e}{b}\right)^2\right]^{-1} ,$$

and C_3, G_3, c and e are defined in Eqs. (A.29), (A.30), and (A.31) respectively.

Expressions (18) and (19) when normalized by $\frac{P}{\pi b^2}\left(\frac{\pi b^2}{\lambda z}\right)^2$ and evaluated as a function of $\frac{kb\rho}{z}$ are only dependent on three parameters. These are the strength of turbulence ϵ, the obscuration ratio δ, and the taper ratio β_o. For the non-focused case this would no longer be true. Indeed, the results would also depend on the Fresnel number $\frac{\pi b^2}{\lambda z}$ and the ratio of the focal range to the propagation range $\frac{f}{z}$.

IV. Numerical Results

The expression for the short-term focused irradiance profile normalized by $\left[\frac{P}{\pi b^2}\left(\frac{\pi b^2}{\lambda z}\right)^2\right]$ for cases $\nu = 1, 2$ have been evaluated numerically. A representative example of the short-term irradiance profile for the truncated obscured gaussian aperture distribution ($\nu = 2$) is presented in Fig. 1 for $\delta = a/b = 0.5$ and $\beta_o = b/\alpha_o = 1$. The curves in this figure are shown for $\epsilon = 2b/\rho_o = 0.1$, 0.25, 0.5, 1.0, 2.5, 5.0, 7.5, and 10.0. For comparison we have plotted, in Fig. 2, the long-term focused irradiance profiles for the same values of parameters used in Fig. 1. From these and other calculated profiles the on-axis irradiance and beam spread may be determined as a function of the strength of turbulence. The on-axis irradiance values computed from the short-term, long-term, and Fried's short-term expressions are shown in Figs. 3, 4, and 5 as a function of ϵ. [In Fig. 3, a uniform amplitude distribution ($\nu = 1$) with an obscuration of 0.5 was used to calculate the three on-axis irradiance curves shown. A truncated gaussian amplitude distribution ($\nu = 2$) with an obscuration of 0.5 and a taper ratio of $\beta_o = 1$ was used

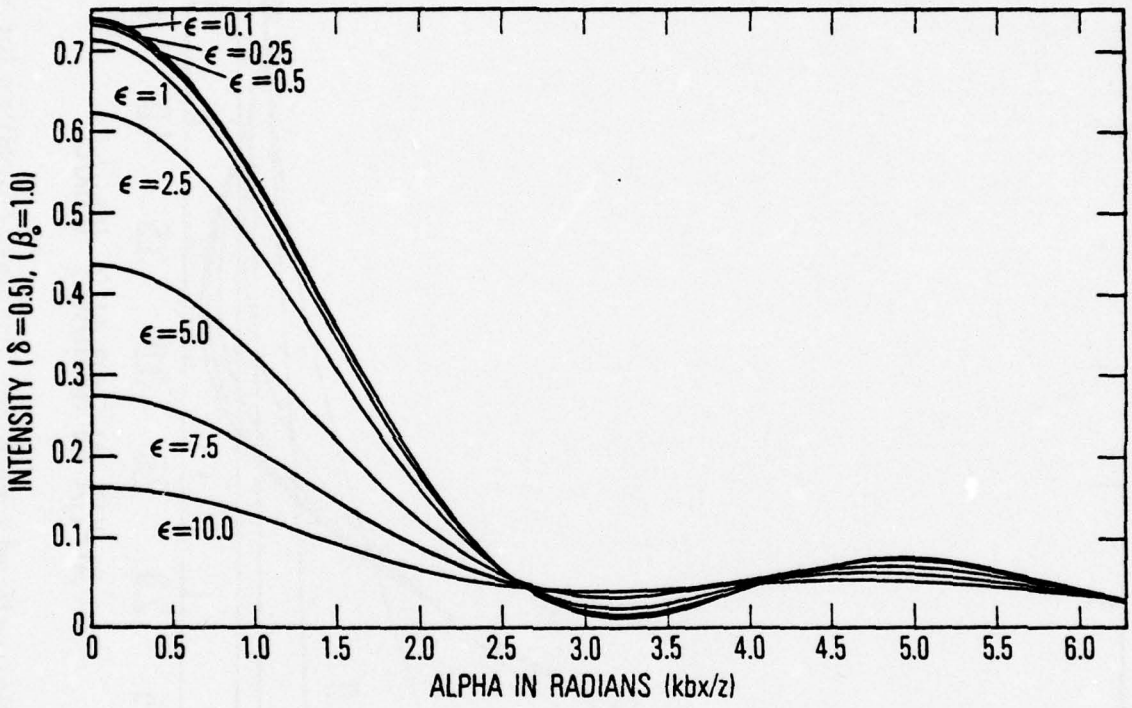

Fig. 1 Normalized short term irradiance profiles for various strength of turbulence values.

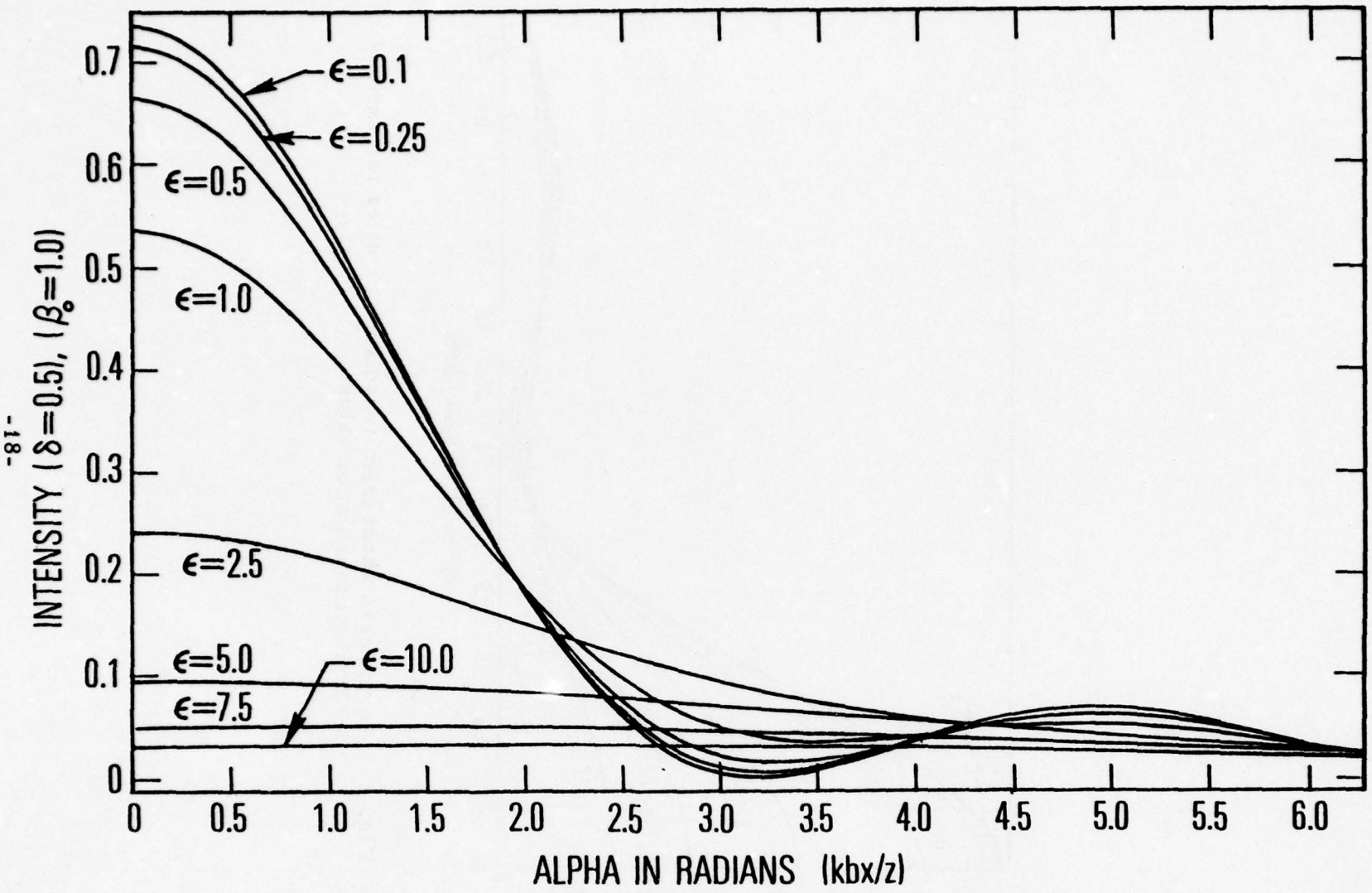

Fig. 2 Normalized long term irradiance profiles for various strength of turbulence values.

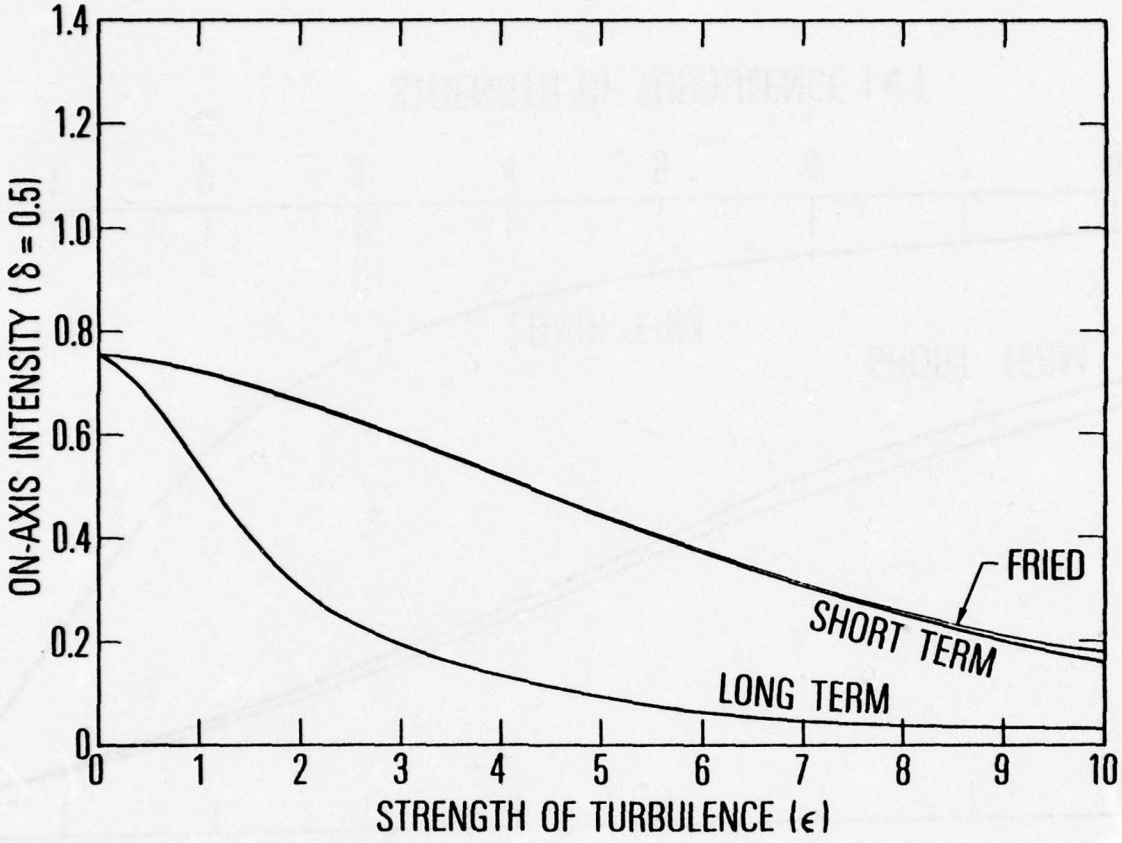

Fig. 3 Normalized on-axis irradiance values using the short term average, long term average, and Fried's approximation to short term average for the MCF. A uniform aperture distribution with an obscuration of 0.5 is used.

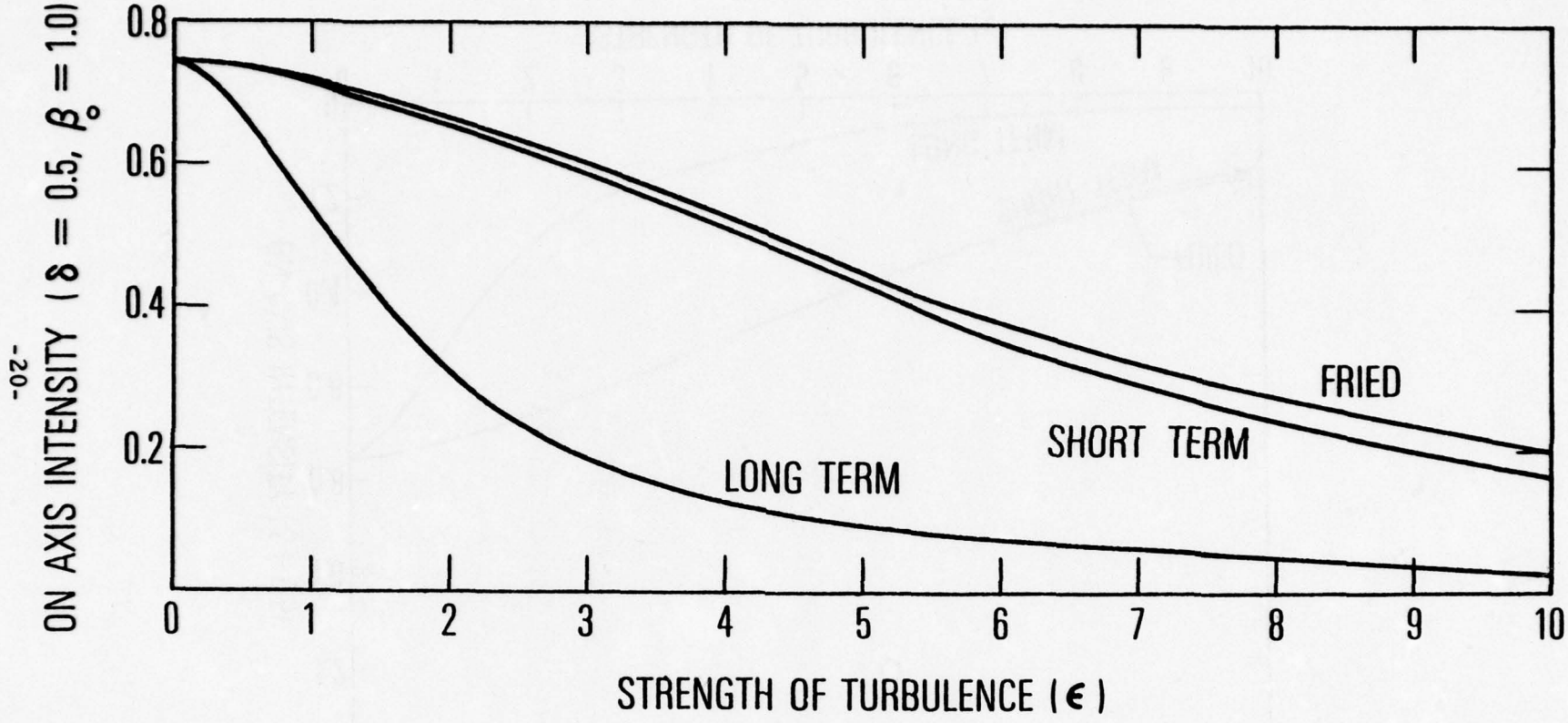

Fig. 4 Normalized on-axis irradiance values using the short term average, long term average, and Fried's approximation to short term average for the MCF. A gaussian aperture distribution with β_o equal to 1.0 and an obscuration of 0.5 is used.

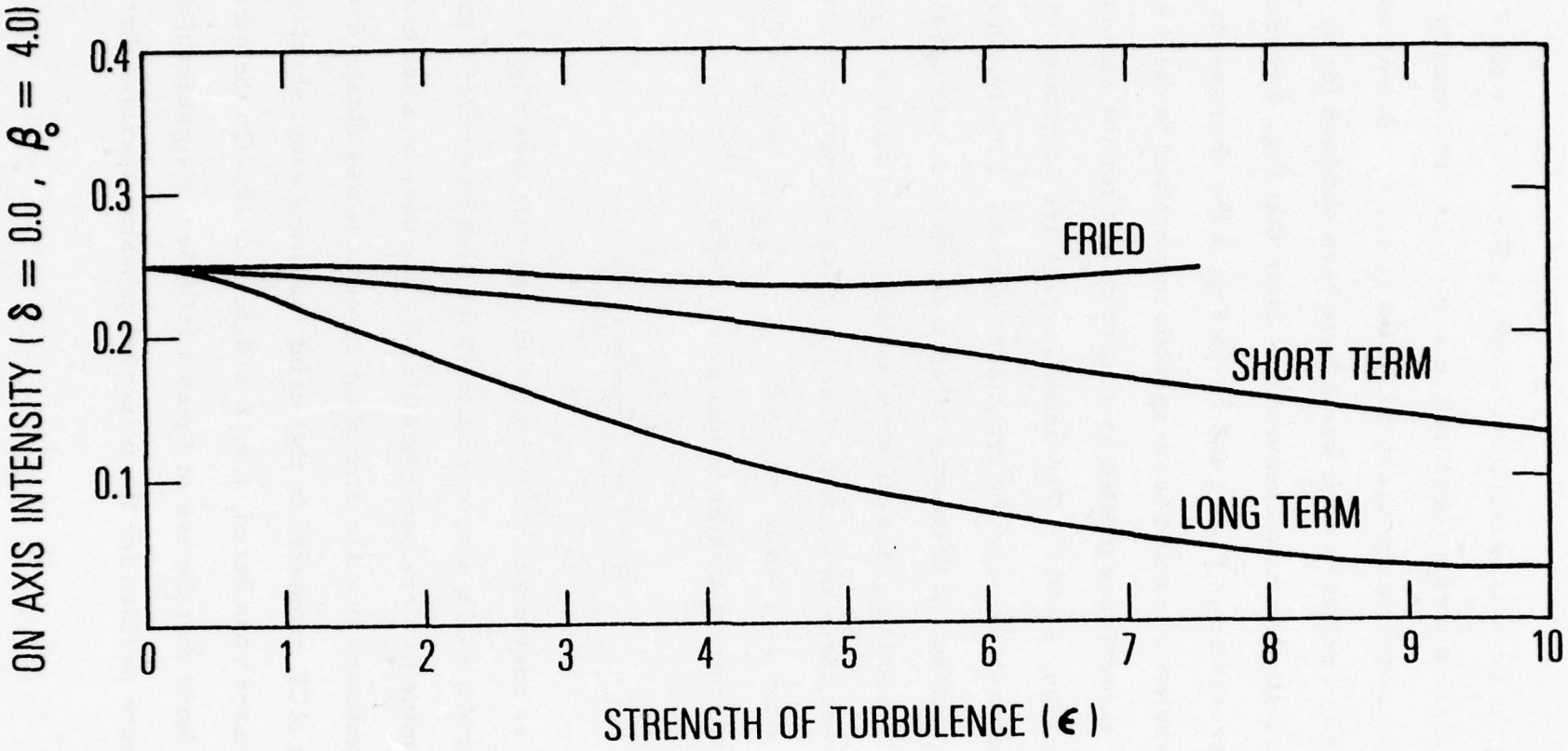

Fig. 5 Normalized on-axis irradiance values using the short term average, long term average, and Fried's approximation to short term average for the MCF. A gaussian aperture distribution with β_o equal to 4.0 and no obscuration is used.

in calculating the on-axis irradiances shown in Fig. 4 while for Fig. 5 a truncated gaussian with no obscuration and a gaussian intensity half-width equal to one-fourth the aperture radius (i.e., $\beta_o = 4$) was used]. This last case is similar to what would have been obtained for an infinite gaussian distribution with no obscuration. Note that Fig. 4 corresponds to the cases presented in Figs 1 and 2. In Fig. 6 the short-term and long-term turbulence induced beam spreads normalized to the $\epsilon = 0$ values (i.e., vacuum) are plotted as a function of ϵ for the same cases considered in Figs. 1 and 2. The beam spreads are determined from 1/e of the maximum value of the irradiance curves. Finally, in Fig. 7 we plot the improvement in on-axis irradiance due to tilt removal (I_{ST}/I_{LT}) as a function of the effective strength of turbulence ϵ_{eff} for several different cases of δ and β_o. The effective strength of turbulence is defined as ϵ for $\nu = 1$ while for $\nu = 2$ $\epsilon_{eff} = D_{eff}/\rho_o$ for $\beta_o \geq 1$ where the effective aperture diameter is that given by Kerr [11]

$$D_{eff} = 4\alpha_o \left(\frac{1 - e^{-\beta_o/2}}{\sqrt{1 - e^{-\beta_o}}} \right)$$

From an analysis of the calculational results (see Fig. 3 - 5), it was found that Fried's approximation to the short-term MCF may be used to determine the irradiance profiles for the case of a uniform aperture distribution ($\nu = 1$). Excellent agreement was obtained when using Fried's MCF compared to that using the more exact short-term MCF for all cases considered, i.e. $\delta \leq 0.5$, $\epsilon \leq 10$. On the other hand, it was found that the use of Fried's MCF led to significant errors in the irradiance profiles for the truncated gaussian aperture distribution

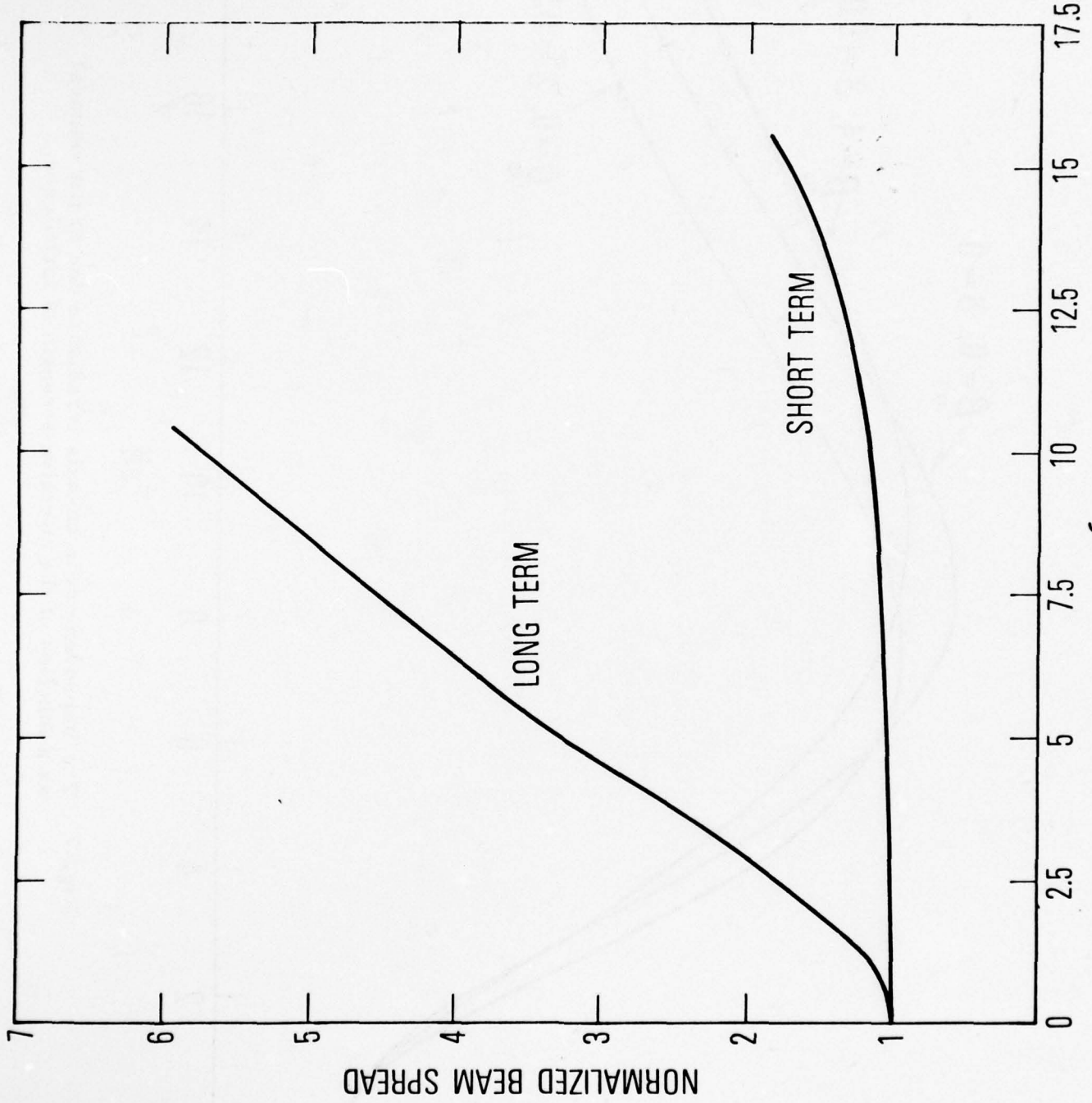

Fig. 6 Normalized beam spreads for the long term and short term irradiance profiles for $\beta_o = 1.0$ and $\delta = 0.5$ as determined from the 1/e point in intensity.

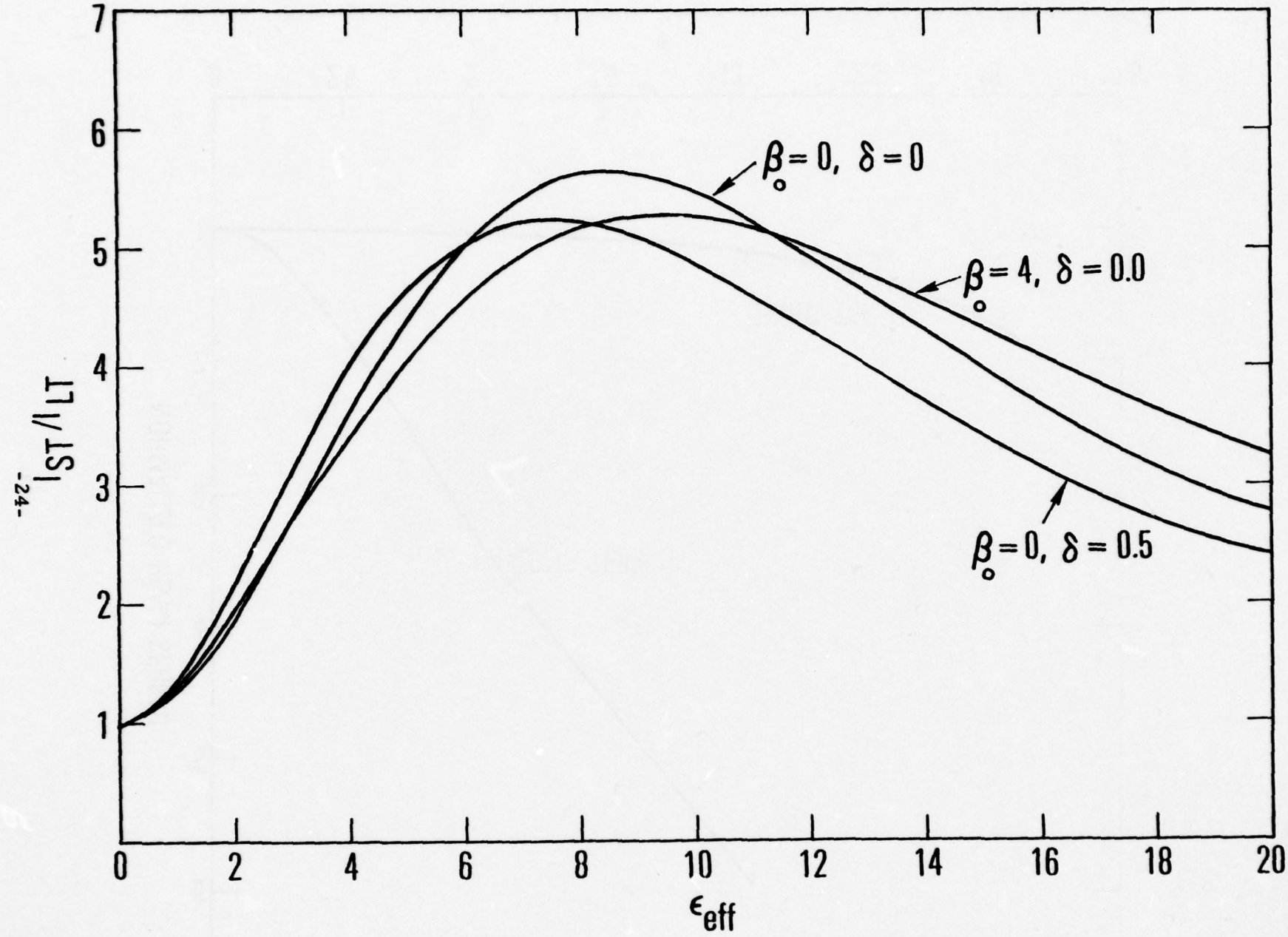

Fig. 7 The improvement in on-axis irradiance due to tilt removal as a function of the effective strength of turbulence.

($\nu = 2$) when $\epsilon \gtrsim 2$ and $\beta_o \gtrsim 2$. In fact for $\beta_o \geq 2$ and $\epsilon \geq 7$, the use of Fried's MCF leads to negative irradiance values.

In Fig. 6 it is seen that long-term beam spread increases in a linear manner with ϵ with a break occurring near $\epsilon = 7$. This change in slope is due to the large obscuration used for the case presented. The linear dependence of long-term beam spread has been noted previously[5]. On the other hand, the short-term average beam spread remains constant, then increases slowly for $\epsilon \gtrsim 5$. In fact, if a different definition of beam spread were used (i.e., the position of the first minimum) the short-term beam spread would remain constant. This short-term beam spread dependence on ϵ has been seen for all cases considered and is in contrast to Ref. 5 where a minimum in the ratio of short to long-term beam spreads is exhibited. In Ref. 5, the short-term beam spread was determined from the short-term lateral coherence length obtained from Fried's approximation to the short-term MCF. In contrast to this previous work, we find that it is in general not possible to characterize the short-term beam spread by an effective short-term lateral coherence length (see below). We also find the recent phenomenological analysis of beam spread presented by Kerr[11] to be somewhat in contrast with the results obtained here. Indeed, Kerr's results imply larger on-axis irradiance values and smaller beam spread angles for $\epsilon \leq 1.69$ than for the turbulence free case.[12] Assuming that Kerr's results apply only for $\epsilon \gtrsim 1.7$, we are lead to beam spreads larger (e.g., factors of two for large values of ϵ) than found in this paper. The present analysis of beam spread indicates that the beam center retains its shape and that the excess energy has been scattered into large angles by the smaller

scales of turbulence. The results then look like the turbulence free irradiance decreased by an extinction coefficient plus the scattered irradiance which has only a weak angular dependence. Therefore as long as the peak extincted irradiance is significantly larger than the peak scattered irradiance, it is not possible to express the short-term beam spread in terms of $z/k\rho_o^{ST}$, where ρ_o^{ST} is a so-called short-term lateral coherence length.[5]

From Fig. 7 it is seen that the irradiance improvement obtained by tilt removal is maximized for $7.5 \leq \varepsilon_{eff} \leq 10$ for the cases considered.† The maximum improvement found was approximately 5.62 for $\nu = 1$. This improvement decreased slowly as β_o increased. Improvement in irradiance for the obscured aperture is less than that for the unobscured cases with maximum improvement occurring at smaller ε_{eff} values. This is not surprising for large obscurations since a large portion of the coherent aperture has been degraded.

In this paper we have written down an expression for the focused short-term irradiance profile for a beam transmitted through a turbulent atmosphere which is valid for a propagation range $z < k\ell^2$. (Recall that ℓ is the smaller of the initial beam diameter D or the long-term spherical wave coherence length.) This expression is more exact but also it is more difficult to calculate numerically than the results obtained by using Fried's approximation.[5] Fortunately it has been found that Fried's approximation can be used with good results to determine the MCF and therefore irradiance profiles for weak to moderate turbulence, $\varepsilon \leq 5$, and for gaussian aperture distributions that are strongly truncated, $\beta_0 \leq 2$.

†Note that $\beta = 0$ indicates the uniform-illumination case. The existence of a maximum in Fig. 7 does not imply the existence of a minimum in the ratio of short term to long term beam spreads using the definition of beam spreads given above.

Finally, we have noted that the short-term average beam spread does not increase with ϵ but remains constant. Obviously this does not hold as ϵ increases without bound, since we have specified that $z < k\ell^2$. Setting $z = k\rho_o^2$, where $\rho_o = (.545\ C_n^2 k^2 z)^{-3/5}$ (Ref. 5), implies that $.545\ C_n^2 = (k^{7/6} z^{11/6})^{-1}$ or $\rho_o = (z/k)^{1/2}$, where C_n^2 is the index of refraction structure constant. This means that if the turbulence becomes so strong (large C_n^2) that ρ_o becomes smaller than the first Fresnel zone for the propagation range z or $\epsilon^2 > kD^2/z$ (the Fresnel number) than the above theory does not hold. When $\epsilon > kD^2/z$ then $\alpha(\rho)$ (see Eq. 5 and following discussion) can no longer be set to unity and must be included rigorously in the determination of D_v.

APPENDIX A

Calculation of the Modified Phase Structure Function for Three Specific Aperture Functions

In this appendix, Eq. (1) is obtained from Eqs. (12) and (16) for the Kolmogorov spectrum and three amplitude aperture functions discussed in the text.

Since we have assumed that $z \ll k\rho^2$, the phase structure function becomes

$$D_\phi(\rho) = 2\,(\rho/\rho_o)^{5/3} \tag{A. 1}$$

where ρ_o is the long-term lateral coherence of a spherical wave length[2]. When ρ is made dimensionless as discussed Section III, Eq. A.1 becomes

$$D_\phi(\rho) = 2\,\varepsilon^{5/3}\,\rho^{5/3} \tag{A. 2}$$

We consider three specific cases.

1) Uniform Aperture Amplitude Distribution With Truncation And Obscuration

Here

$$\begin{aligned} W_1(r) &= 1 \qquad a \le |r| \le b \\ &= 0 \qquad 0 \le |r| < a \\ &\qquad\quad |r| > b \end{aligned} \tag{A. 3}$$

where "b" is the aperture (truncation) radius, and a the obscuration radius. First, Eq. (16) is rewritten as

$$D_\gamma(\vec{\rho}, \vec{R}) = D_\phi(\rho) - X_1(\rho) + Y_1(\vec{\rho}, \vec{r}_1) - Y_1(\vec{\rho}, \vec{r}_2) \quad , \tag{A. 4}$$

where $\vec{r}_{1,2} = \vec{R} \pm \frac{\vec{\rho}}{2}$ and $X_1(\rho)$, $Y_1(\vec{\rho}, r_{1,2})$ is the second and third term of Eq. (16), respectively. Substituting Eq. (A.3) into Eq. (15) yields

$$A_1 = \frac{4}{\pi b^4} \left(1 - \delta^4\right)^{-1} , \tag{A.5}$$

where

$$\delta = b/a$$

Upon substituting Eq. (A.1) and (A.3) into (A.4) Y_1 becomes

$$Y_1(\vec{\rho}, \vec{r}_1) = \frac{2 A_1 \vec{\rho} \cdot \vec{r}_1}{\rho_o^{5/3} r_1^2} \int_0^{2\pi} \int_a^b \vec{r} \cdot \vec{r}_1 \left|\vec{r} - \vec{r}_1\right|^{5/3} r dr d\theta \tag{A.6}$$

Upon performing the angular integration, using the series expansion for the Hypergeometric function[12], and expressing the results in terms of dimensionless variables, Eq. (A.6) becomes

$$Y_1(\vec{\rho}, \vec{r}_1) = -2 \left(\frac{\epsilon}{2}\right)^{5/3} \vec{\rho} \cdot \vec{r}_1 \; G_1(r_1, \delta) \tag{A.7}$$

where

$$G_1(r_1, \delta) = \frac{40}{3} \left(1 - \delta^4\right)^{-1} \int_\delta^1 \frac{r^3}{(r_1 + r)^{1/3}} F\left(\frac{1}{6}, \frac{3}{2}, 3 \frac{4 r r_1}{(r_1 + r)^2}\right) dr \tag{A.8}$$

and F is the Hypergeometric function of the indicated variables. To proceed further, Eq. (A.8) must be evaluated numerically

From Eqs. (16), (A.1), (A.3), and (A.4) we obtain

$$X_1(\rho) = \frac{A_1^2 \rho^2}{2 \rho_o^{5/3}} \int_0^{2\pi} \int_a^b \int_0^{2\pi} \int_a^b \vec{r} \cdot \vec{r}' \left|\vec{r} - \vec{r}'\right|^{5/3} r dr \, r' dr' \, d\theta \, d\theta' \tag{A.9}$$

To evaluate this fourth degree integral a change of variables is made from $\vec{r}$, $\vec{r}'$ to the sum and difference coordinates $\vec{\eta} = \frac{\vec{r} + \vec{r}'}{2}$ and $\vec{\xi} = \vec{r} - \vec{r}'$ respectively. The range of integration of $\vec{\xi}$ is over a circle of radius 2b while the range of integration of $\vec{\eta}$ is over the overlap area of two circles of radius "b" and obscuration radius "a" whose centers are separated by a distance of ξ. Since the amount of overlap and obscuration changes with ξ, Eq. (A.9) is broken into four terms to account for the differing dependence on ξ. These represent: 1) For $0 \leq \xi \leq 2b$, the overlap area of two circles of radius b separated by a distance ξ; 2) For $0 \leq \xi \leq b + a$, the removal of the obscuration areas from the two circles of radius b (for $\xi > b + a$ there is no obscuration within the overlap area of two circles); 3) For $0 \leq \xi \leq 2a$, the addition of the overlap area of the obscuration circles of radius "a" since this area was removed twice (incorrectly) in 2 (there is no overlap of the obscuration areas for $\xi > 2a$; and 4) For $b - a \leq \xi \leq b + a$, the addition of the obscuration areas outside of the overlap area of the circles of radius b. Figure A-1 is a geometric representation of the integration area for the $\vec{\eta}$ variable. Note that in Fig. A.1-b the obscuration area is shown non-overlapped for clarity.

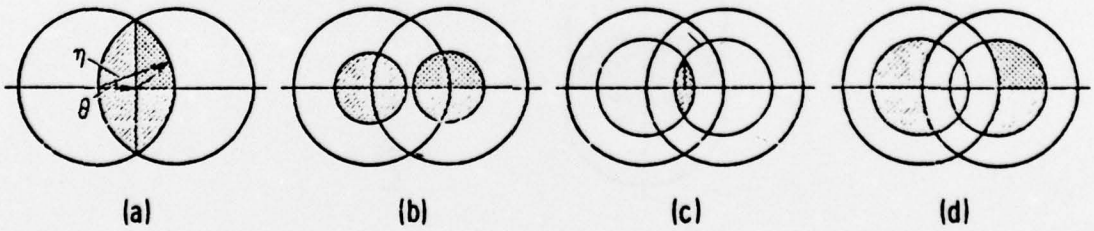

Fig. A-1 Geometric Representation of Aperture Overlap Area for the Integration Variable η

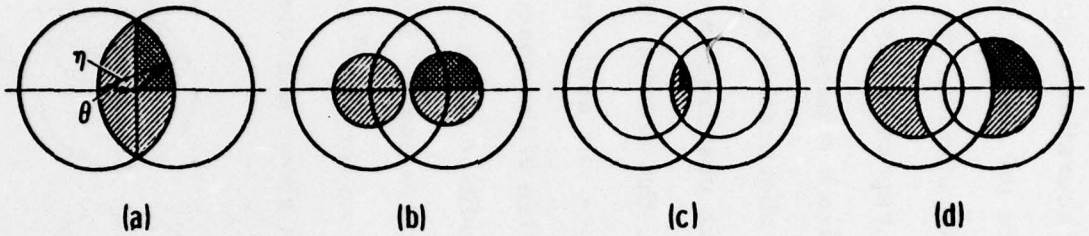

Fig. A-1 Geometric representation of aperture overlap area for the integration variable η.

From the above discussion and upon performing the angular integration in $\vec{\xi}$ immediately, X_1 can be expressed in terms of dimensionless variables (ξ and η divided by 2b and b, respectively) as

$$X_1 = 64\pi b^8 A_1^2 (\epsilon)^{5/3} (I_1 + I_2 + I_3 + I_4) \tag{A. 10}$$

where the I_i correspond to the terms discussed above and the corresponding geometry is exhibited in Fig. A-1. The integration is over the double crossed hatched area in Fig. A-1 through symmetry of the angular variables. The relevant integrals I_i are given by

$$I_1 = \int_{\delta}^{1} \xi^{8/3} d\xi \int_{0}^{\cos^{-1}\xi} d\theta \int_{\xi \sec\theta}^{1} (\eta^2 - 2\eta\xi\cos\theta)\, \eta d\eta$$

$$= -\frac{\sqrt{\pi}\,\Gamma\left(\frac{4}{3}\right)}{\Gamma\left(\frac{11}{6}\right)} \quad \frac{180}{47311} \tag{A. 11}$$

where by a change in variables $\vec{\eta}$ is now centered in the left-hand circle of Fig. A-1 a and Γ represents the gamma function. The second integral appearing in Eq. (A. 10) is given by

$$I_2 = -\int_{0}^{\frac{1+\delta}{2}} \xi^{8/3} d\xi \int_{0}^{\pi} d\theta \int_{\tilde{0}}^{\delta} \eta d\eta (\eta^2 + 2\xi\eta\cos\theta)$$

$$= -\frac{3\pi}{44} \delta^4 \left(\frac{1+\delta}{2}\right)^{11/3} \tag{A. 12}$$

where the variable $\vec{\eta}$ is centered in the right-hand circle of Fig. A-1.b and the integration is performed over the top right half obscuration area. The third integral in (A. 10) is similar to the first except that $0 \le \xi \le \delta$. This integral is

given by

$$I_3 = \int_0^{\delta} \xi^{8/3}\, d\xi \int_0^{\cos^{-1}\xi/\delta} d\theta \int_{\xi\cos\theta}^{\delta} (\eta^2 - 2\eta\,\xi\cos\theta)\eta\, d\eta \qquad (A.13)$$

$$= \delta^{23/3} I_1$$

In order to analytically reduce the integral occurring in I_4, the integration area in $\overline{\eta}$ (Fig. A-1 d) is broken into two terms described schematically in Fig. A-2.

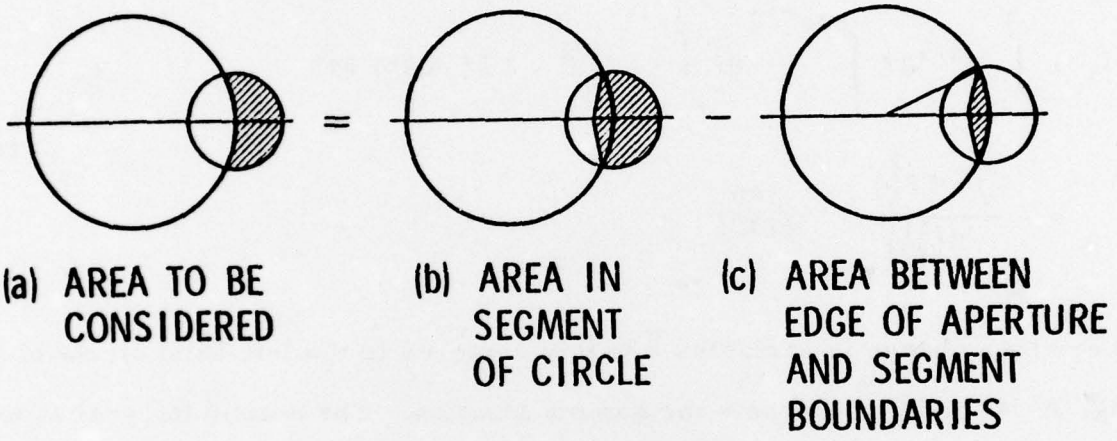

Fig. A-2 Schematic of the Integration Area for the η Variable in Fig. A-1 d

Using this division I_4 is written as

$$I_4 = \int_{\frac{1-\delta}{2}}^{\frac{1+\delta}{2}} \xi^{8/3}\, d\xi \left\{ \int_0^{\alpha} d\theta \int_0^{\delta} (\eta^2 + 2\xi\,\eta\cos\theta)\,\eta\, d\eta \right. \qquad (A.14)$$

$$\left. - \int_0^{\overline{\theta}} d\theta \int_{2\,\xi\sin\alpha\csc\varphi}^{1} (\eta^2 - 2\xi\,\eta\cos\theta)\eta\, d\eta \right\}$$

where

$$\alpha = \cos^{-1}\left(\frac{1 - 4\xi^2 - \delta^2}{4\delta\xi}\right), \quad \overline{\theta} = \cos^{-1}\left(\frac{1 + 4\xi^2 - \delta^2}{4\xi}\right), \quad \varphi = \alpha - \theta \quad ,$$

The first term in the integration over $\vec{\eta}$ is shown schematically in Fig. A-2b (the origin of the $\vec{\eta}$ integration is at the center of the obscuration circle) and the second term is represented by Fig. A-2c, (the origin of the $\vec{\eta}$ integration is at the center of the large circle).

On performing the inner integrations, Eq. (A.14) becomes

$$I_4 = \frac{1}{4} \int_{\frac{1-\delta}{2}}^{\frac{1+\delta}{2}} \xi^{8/3} \, d\xi \; T(\xi, \overline{\theta}, \alpha, \overline{\varphi}) \qquad \text{(A.15)}$$

where

$$T(\xi, \overline{\theta}, \alpha, \varphi) = \delta^4 \alpha + \frac{8}{3}\delta^3 \xi \sin\alpha - \overline{\theta} + \frac{8}{3}\xi \sin\overline{\theta}$$

$$+ 16\,\xi^4 \sin^4\alpha \left(\operatorname{ctn}\overline{\varphi} - \operatorname{ctn}\alpha + \frac{\operatorname{ctn}^3\overline{\varphi} - \operatorname{ctn}^3\alpha}{3}\right)$$

$$- \frac{64}{3}\xi^4 \sin^3\alpha \left[\frac{\cos\alpha}{2}\left(\csc^2\overline{\varphi} - \csc^2\alpha\right) + \sin\alpha\left(\operatorname{ctn}\overline{\varphi} - \operatorname{ctn}\alpha\right)\right],$$

and $\overline{\varphi} = \alpha - \overline{\theta}$. To proceed further, Eq. (A.15) must be computed numerically. In terms of the dimensionless variable ρ, $X(\rho)$ is then written as

$$X(\rho) = -2\,C_1\,\varepsilon^{5/3}\,\rho^2 \qquad \text{(A.16)}$$

where

$$C_1 = \frac{2^9}{\pi}(1-\delta^4)^{-2}\left[\left(\frac{\pi^{1/2}\,\Gamma\left(\frac{4}{3}\right)}{\Gamma\left(\frac{11}{6}\right)}\,\frac{180}{47311}\right)\left(1+\delta^{\frac{23}{3}}\right)\right. \tag{A.17}$$

$$\left. + \frac{3\pi}{44}\left(\frac{1+\delta}{2}\right)^{11/3}\delta^4 - 1/4\int_{\frac{1-\delta}{2}}^{\frac{1+\delta}{2}} \xi^{8/3}\, T(\xi,\overline{\theta},\alpha,\overline{\varphi})\, d\xi\right]$$

From Eqs. (5), (12), (16), (A. 1), (A. 3), (A. 4), (A. 7), and (A. 17) the short-term MCF for the uniform amplitude aperture distribution, in terms of dimensionless variables, is given by

$$M_{ST} = \exp\left\{-\varepsilon^{5/3}(\rho^{5/3} + C_1\rho^2)\right. \tag{A.18}$$

$$\left. + \left(\frac{\varepsilon}{2}\right)^{5/3}[\vec{\rho}\cdot\vec{r}_1\, G_1(r_1) - \vec{\rho}\cdot\vec{r}_2\, G_1(r_2)]\right\}$$

When Fried's approximation is made[7], the sign of C_1 is changed and G_1 is set to zero. However, the resulting expression does not agree with the results found in Eq. (10) Ref. 5. Reference 5 appears to be incorrect due to two errors. The first is a calculational error in determining Eq. (5) Ref. 5 and the second is the replacement of ρ by ρt and integration of t from 0 to 1 in the determination of tilt removal to account for the difference between plane and spherical wave propagation. This effect had already be accounted for in the long-term phase structure function and was included numerically into the long term phase coherence length ρ_o. This can also be seen by referring to Ref. 4, Eqs. (26) - (28).

2) Gaussian Aperture Amplitude Distribution with Truncation and Obscuration

For this case the unnormalized aperture function is given by

$$W_2 = e^{-r^2/\alpha_o^2} \qquad a \le |r| \le b$$
$$= 0 \qquad \text{otherwise} \tag{A.19}$$

where α_o is a measure of the 1/e point in irradiance. The normalization "A_2" is obtained from Eqs. (15) and (A.19) as

$$A_2 = \left(\pi \int_a^b r^3 \, e^{-r^2/\alpha_o^2} \, dr \right)^{-1}$$

$$= 2 \left[\beta_o \left(\delta^2 \, e^{-(\delta\beta_o)^2} - e^{-\beta_o^2} \right) + e^{-(\delta\beta_o)^2} - e^{-\beta_o^2} \right]^{-1} \Big/ (\pi b^4 \beta_o^4)$$

and the symbol β_o is used to represent b/α_o. Without going into as much explanation as was used in presenting Eq. (A.7) and (A.16) for the uniform case, we write

$$G_2(r_1) = \frac{20}{3} \beta_o^4 \left[\beta_o^2 \left(\delta^2 e^{-(\delta\beta_o)^2} - e^{-\beta_o^2} \right) + e^{-(\delta\beta_o)^2} - e^{-\beta_o^2} \right]^{-1}$$
$$\times \int_\delta^1 \frac{r^3}{(r + r_1)^{1/3}} \, e^{-r^2\beta_o^2} \, F\left(\frac{1}{6}, \frac{3}{2}, 3, \frac{4 r r_1}{(r + r_1)^2} \right) dr \tag{A.20}$$

and

$$C_2 = \frac{32}{\pi} \beta_o^6 \left[\beta_o^2 \left(\delta^2 e^{-(\delta\beta_o)^2} - e^{-\beta_o^2} \right) + e^{-(\delta\beta_o)^2} - e^{-\beta_o^2} \right]^{-2} \sum_{i=1}^{5} I_i \tag{A.21}$$

The I_i terms represent integrals for which the integration area for the η variable is the same as that discussed above for Eqs. (A.11) - (A.15) and Fig. A.1). Different choices are made for the order of integration to

analytically reduce the integrals. Therefore

$$I_1 = \int_0^1 \xi^{8/3}\, d\xi\, e^{-2\beta_o^2\xi^2} \left\{ \left[\int_0^{\pi/2} e^{-2\beta_o^2 R_1^2} \left(R_1^2 + \frac{1}{2\beta_o^2} - \xi^2 \right) d\theta \right] - \frac{\pi}{2} \left(\frac{1}{2\beta_o^2} - \xi^2 \right) \right\} \quad \text{(A.22)}$$

where

$$R_1 = \xi \cos\theta + \sqrt{1 - \xi^2 \sin^2\theta}$$

Equation (A.22) is equivalent to Eq. (A.11) though an integration over $\vec{\eta}$ has been performed and a factor of $-(4\beta_o^2)^{-1}$ removed from the integral. Further, the origin of the $\vec{\eta}$ integration is at the center of the overlap area of the two large circles in Fig. A-1a. The integral I_2 has an $\vec{\eta}$ integration over the overlap area of the obscuration and is found in a manner similar to that used in obtaining Eq. (A.22) (See Eq. (A.13) and Fig. A-1c). The results are

$$I_2 = \int_0^{\delta} \xi^{8/3}\, d\xi\, e^{-2\beta_o^2\xi^2} \left\{ \left[\int_0^{\pi/2} e^{-2\beta_o^2 R_2^2} \left(R_2^2 + \frac{1}{2\beta_o^2} - \xi^2 \right) d\theta \right] - \frac{\pi}{2} \left(\frac{1}{2\beta_o^2} - \xi^2 \right) \right\} \quad \text{(A.23)}$$

where

$$R_2 = -\xi \cos\theta + \sqrt{\delta^2 - \xi^2 \sin^2\theta}$$

The integral I_3 is calculated in a manner similar to that used in calculating Eq. (A.12) except that here a different aperture function W has been used and that the dimensionless variable ξ is now integrated between 0 and $\sqrt{1 + 3\delta^2}/2$. The reason for this is that it is difficult to express an integral for the obscuration area outside of the overlap area of the large circles which is reducible analytically for ξ greater than $\sqrt{1 + 3\delta^2}/2$. This upper limit in ξ is determined by the intersection of the large circle with the

obscuration circle such that $\vec{\eta}$ (from the center of the overlap area) is tangent to the obscuration circle at that point. With the angular integration over $\vec{\eta}$ performed (here from the center of the obscuration circle) we obtain

$$I_3 = 4\pi\beta_o^2 \int_0^{\frac{\sqrt{1+3\delta^2}}{2}} \xi^{8/3} d\xi\, e^{-2\beta_o^2\xi^2} \int_0^{\delta} \eta d\eta\, e^{-2\beta_o^2(\eta-\xi)^2} \left[\eta^2 \bar{I}_0(4\beta_o^2\eta\xi) - 2\xi\eta\bar{I}_1(4\beta_o^2\eta\xi)\right] \tag{A.24}$$

where $\bar{I}_i(x) = e^{-x} I_i(x)$ and $I_i(x)$ is modified Bessel function of order i.[12] (Do not confuse $I_i(x)$ with symbols I_i above). The integral I_4 represents the same quantity calculated in Eqs. (A.14) and (A.15) except that the upper limit on ξ is $\sqrt{1+3\delta^2}/2$ and that the origin of the $\vec{\eta}$ integration is the center of the overlap area. Upon performing the η integration we obtain

$$I_4 = \int_{\frac{1-\delta}{2}}^{\frac{\sqrt{1+3\delta^2}}{2}} \xi^{8/3} d\xi\, e^{-2\beta_o^2\xi^2} \int_0^{\alpha} d\theta \left[\left(R_3^2 - \xi^2 + \frac{1}{2\beta_o^2}\right) e^{-2\beta_o^2 R_3^2} - \left(R_1^2 - \xi^2 + \frac{1}{2\beta_o^2}\right) e^{-2\beta_o^2 R_1^2}\right] , \tag{A.25}$$

where again a factor of $(4\beta_o^2)^{-1}$ has been removed and included in the constant terms of Eq. (A.21) and

$$\begin{aligned} R_3 &= \xi\cos\theta + \sqrt{\delta^2 - \xi^2\sin^2\theta} \\ \alpha &= \sin^{-1}\left(\frac{\sin\gamma}{Z}\right) \\ \gamma &= \cos^{-1}\left(\frac{1+4\xi^2-\delta^2}{4\xi}\right), \quad Z = \sqrt{1+\xi^2-2\xi\cos\gamma} \end{aligned} \tag{A.26}$$

Finally, for $\sqrt{1+3\delta^2}/2 \le \xi \le (1+\delta)/2$ the integral I_5 corresponds to that part of the obscuration area inside the overlap of the large circles. The resulting integral, upon performing the η integration, is

$$I_5 = -\int_{\frac{\sqrt{1+3\delta^2}}{2}}^{\frac{1+\delta}{2}} \xi^{8/3} d\xi\, e^{-2\beta_o^2\xi^2} \int_0^{\alpha} d\theta \left[\left(R_1^2 - \xi^2 + \frac{1}{2\beta_o^2}\right) e^{-2\beta_o^2 R_1^2} - \left(R_4^2 - \xi^2 + \frac{1}{2\beta_o^2}\right) e^{-2\beta_o^2 R_4^2}\right] \tag{A.26}$$

where $R_4 = -R_2$.

The MCF for this case is obtained from Eq. (A.18) by replacing G_1, C_1 by G_2 and C_2, respectively.

3) Infinite Gaussian Aperture Amplitude Distribution with Semi-Gaussian Obscuration

The appropriate unnormalized aperture function that was used is given by

$$W_3 = e^{-r^2/b^2}\left(1 - e^{-r^2/a^2}\right)^2 , \tag{A.27}$$

where b represent the gaussian halfwidth.

This is an unusual aperture function and was chosen so that the expression for the irradiance profile (Eq. 19) is easily expressible in terms of $\vec{\rho}$, $\vec{R}$. For this aperture function the determination of the modified phase structure function is simplified since the integrations occurring in Eq. (A.4) are carried out over all space. The appropriate normalization

constant A_3, G_3 and C_3 are listed below

$$A_3 = 2\left[1 - 2\left(\frac{c}{b}\right)^4 + \left(\frac{e}{b}\right)^4\right]^{-1} / (\pi b^4) \qquad \text{(A.28)}$$

$$G_3(r_1) = \frac{10}{3}\,\Gamma\left(\frac{11}{6}\right)\left[1 - 2\left(\frac{c}{b}\right)^4 + \left(\frac{e}{b}\right)^4\right]^{-1}$$

$$\times\left[M\left(\frac{1}{6}, 2, -r_1^2\right) - 2\left(\frac{c}{b}\right)^{\frac{11}{6}} M\left(\frac{1}{6}, 2, -\left(\frac{b\,r_1}{c}\right)^2\right) + \left(\frac{e}{b}\right)^{\frac{11}{6}} M\left(\frac{1}{6}, 2, -\left(\frac{b r_1}{e}\right)^2\right)\right] \qquad \text{(A.29)}$$

where $M(a, b, x)$ is the confluent hypergeometric function[13] and

$$C_3 = \frac{5}{6}\,2^{1/6}\,\Gamma\left(\frac{11}{6}\right)\left[1 - 2\left(\frac{c}{b}\right)^4 + \left(\frac{e}{b}\right)^4\right]^{-2}$$

$$\times\left\{1 + \frac{24}{5}\left(\frac{d}{b}\right)^4\left(\frac{g}{b}\right)^{\frac{11}{6}}\left[1 - \frac{11}{6}\left(\frac{g}{d}\right)^2\left(1 - \frac{d^4}{4a^4}\right)\right] + 4\left(\frac{c}{b}\right)^{\frac{23}{3}}\right. \qquad \text{(A.30)}$$

$$\left. + \frac{24}{5}\left(\frac{f}{b}\right)^4\left(\frac{h}{b}\right)^{\frac{11}{3}}\left[1 - \frac{11}{6}\left(\frac{h}{f}\right)^2\left(1 - \frac{f^4}{4a^4}\right)\right] + \left(\frac{e}{b}\right)^{\frac{23}{3}}\right\}$$

In the above

$$\frac{1}{c^2} = \frac{1}{b^2} + \frac{1}{a^2},\quad \frac{1}{d^2} = \frac{1}{b^2} + \frac{1}{2a^2},\quad \frac{1}{e^2} = \frac{1}{b^2} + \frac{2}{a^2},\quad \frac{1}{f^2} = \frac{1}{b^2} + \frac{3}{2a^2},$$

$$\frac{1}{g^2} = \frac{1}{d^2} - \frac{d^2}{4a^4},\quad \frac{1}{h^2} = \frac{1}{f^2} - \frac{f^2}{4a^4}$$

Again, C_3, G_3 are substituted for C_1, G_1 in Eq. (A.18) to obtain the short term MCF.

REFERENCES

1. W. P. Brown, J. Opt. Soc. Am. 61, 1051 (1971).
2. R. F. Lutomirski and H. T. Yura, Appl. Opt. 10, 1652 (1971).
3. H. T. Yura, Appl. Opt. 10, 2771 (1971).
4. A. I. Kon, Izv, Vyssh. Vchebn Zaved. Radiofiz. 13, 61 (1970).
5. H. T. Yura, J. Opt. Soc. Am. 63, 567 (1973).
6. C. Hogge, Private communication.
7. D. L. Fried, J. Opt. Soc. Am. 56, 1372 (1966).
8. R. F. Lutomirski and H. T. Yura, J. Opt. Soc. Am. 59, 99 (1969).
9. V. I. Tatarskii, "Wave Propagation in a Turbulent Medium, (McGraw-Hill Book Co., New York, New York, 1961).
10. D. L. Fried, J. Opt. Soc. Am. 55, 1427 (1965).
11. J. R. Kerr, AGARD Conference on Optical Propagation in the Atmosphere, pp. 21-1, October 1975.
12. J. R. Kerr, private commun. Dr. Kerr has recently modified his results to take this into account.

THE IVAN A. GETTING LABORATORIES

The Laboratory Operations of The Aerospace Corporation is conducting experimental and theoretical investigations necessary for the evaluation and application of scientific advances to new military concepts and systems. Versatility and flexibility have been developed to a high degree by the laboratory personnel in dealing with the many problems encountered in the nation's rapidly developing space and missile systems. Expertise in the latest scientific developments is vital to the accomplishment of tasks related to these problems. The laboratories that contribute to this research are:

Aerophysics Laboratory: Launch and reentry aerodynamics, heat transfer, reentry physics, chemical kinetics, structural mechanics, flight dynamics, atmospheric pollution, and high-power gas lasers.

Chemistry and Physics Laboratory: Atmospheric reactions and atmospheric optics, chemical reactions in polluted atmospheres, chemical reactions of excited species in rocket plumes, chemical thermodynamics, plasma and laser-induced reactions, laser chemistry, propulsion chemistry, space vacuum and radiation effects on materials, lubrication and surface phenomena, photosensitive materials and sensors, high precision laser ranging, and the application of physics and chemistry to problems of law enforcement and biomedicine.

Electronics Research Laboratory: Electromagnetic theory, devices, and propagation phenomena, including plasma electromagnetics; quantum electronics, lasers, and electro-optics; communication sciences, applied electronics, semiconducting, superconducting, and crystal device physics, optical and acoustical imaging; atmospheric pollution; millimeter wave and far-infrared technology.

Materials Sciences Laboratory: Development of new materials; metal matrix composites and new forms of carbon; test and evaluation of graphite and ceramics in reentry; spacecraft materials and electronic components in nuclear weapons environment; application of fracture mechanics to stress corrosion and fatigue-induced fractures in structural metals.

Space Sciences Laboratory: Atmospheric and ionospheric physics, radiation from the atmosphere, density and composition of the atmosphere, aurorae and airglow; magnetospheric physics, cosmic rays, generation and propagation of plasma waves in the magnetosphere; solar physics, studies of solar magnetic fields; space astronomy, x-ray astronomy; the effects of nuclear explosions, magnetic storms, and solar activity on the earth's atmosphere, ionosphere, and magnetosphere; the effects of optical, electromagnetic, and particulate radiations in space on space systems.

THE AEROSPACE CORPORATION
El Segundo, California

• • •